Journal of Applied Polymer Science

Facile UV-curing technique to establish a 3D-grafted poly(ethylene glycol) layer on an epoxy resin base for underwater applications

Yang Yang,[1] Huali Luo,[1] Jinlong Yang,[2] Daofen Huang,[2] Shuxue Zhou[1]

[1]Department of Materials Science, State Key Laboratory of Molecular Engineering of Polymers, Advanced Coatings Research Center of Ministry of Education of China, Fudan University, Shanghai 200433, China

[2]Key Laboratory of Exploration and Utilization of Aquatic Genetic Resources, Shanghai Ocean University, Ministry of Education, Shanghai 201306, China

Correspondence to: S. Zhou (E-mail: zhoushuxue@fudan.edu.cn)

ABSTRACT: Construction of a highly hydrophilic polymer surface with excellent long-term stability underwater is a great challenge. In this paper, a facile ultraviolet (UV) curing technique was employed to realize the three-dimensional (3D) grafting of poly(ethylene glycol) diacrylate (PEGDA, molecular weight: 400, 600, and 1000 g/mol) on a bisphenol A epoxy acrylate (BEA) sheet. The cross section morphology, surface chemical composition, and wettability of the sheets were monitored using an optical microscope, an attenuated total reflectance Fourier transform infrared spectroscope, and a water contact angle analyzer, respectively. The PEGDA-grafted epoxy sheets displayed a highly hydrophilic surface and meanwhile possessed excellent stability underwater, despite the molecular weight of PEGDA. In contrast, the PEGDA/BEA blend sheets are easily damaged underwater, due to strong swelling. In addition, the PEGDA1000-grafted BEA sheet demonstrated good antifouling performance in a natural marine environment. Nevertheless, its long-term antifouling is not satisfactory, being presumably due to hydrolysis or biodegradation of the PEG segments. © 2016 Wiley Periodicals, Inc. J. Appl. Polym. Sci. **2016**, *133*, 43972.

KEYWORDS: applications; coatings; grafting; hydrophilic polymers

Received 11 March 2016; accepted 22 May 2016
DOI: 10.1002/app.43972

INTRODUCTION

Traditional antifouling coatings usually containing organic tin compounds or biopesticides are poisonous and easily enriched in the food chain, causing serious environmental and safety issues. These antifouling coatings are banned worldwide by laws and regulations. Currently, antifouling coatings are mainly based on Cu_2O. However, the Cu_2O-based coatings are still toxic to marine creatures and will be prohibited in the future. Development of nontoxic antifouling coatings is thus urgently demanded.

The nontoxic antifouling coatings include fouling-release coatings with low surface energy, bioinspired micro/nanostructured coatings, nonfouling coatings based on hydrophilic polymers, zwitterionic polymers, and peptoids.[1] In particular, nonfouling coatings (or surfaces) based on poly(ethylene glycol) (PEG) are frequently reported.[2–14] To date, there are two main forms, PEG brushes and PEG-based hydrogels, used in the fabrication of antifouling coatings or surfaces.[6]

For example, Efremova *et al.*[15] prepared PEG brushes on hydrophobized mica by Langmuir–Blodgett deposition to elucidate the interaction between protein and a PEG brush. He *et al.*[16] grafted PEG brushes onto the surfaces and pore walls of α-Al_2O_3 membranes by surface-initiated atom-transfer radical polymerization and improved the protein resistance of the membranes. Sun *et al.*[17] presented poly(vinylidenefluoride-hexafluoropropylene) nanofiber membranes with improved hydrophilicity and protein-fouling resistance through atmospheric pressure glow discharge plasma pretreatment of the membrane and subsequent graft copolymerization of poly(ethylene glycol) methyl ether methacrylate (PEGMA). Kingshott *et al.*[10] treated perfluorinated poly(ethylene-*co*-propylene) tape and poly(ethylene terephthalate) sheets with thin amine polymer layers using radio frequency glow discharge and further grafted methoxy-terminated aldehyde-PEG and dialdehyde-PEG onto the aminated surfaces by reductive amination to minimize multicomponent protein adsorption. Higuchi *et al.*[11] physically attached polyethylene oxide–polypropylene oxide–polyethylene oxide triblock copolymers to the polysulfone membranes to suppress protein and platelet adsorption. Statz *et al.*[12] modified a Ti surface with methoxy-terminated PEG and showed a substantial decrease in attachment of both *Navicula* cells and *Ulva* zoospores. Khalila *et al.*[18] designed PEG-conjugated triscatecholates,

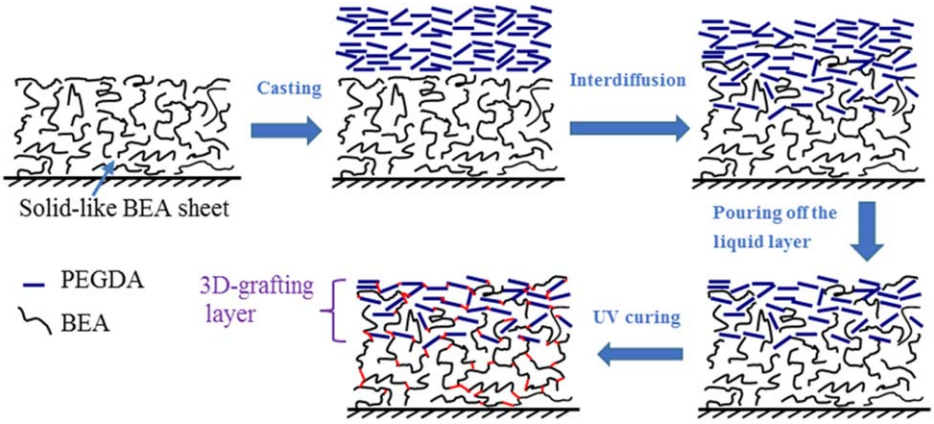

Figure 1. Schematic diagram of preparation of PEGDA-grafted BEA sheets. [Color figure can be viewed in the online issue, which is available at wileyonlinelibrary.com.]

then coated them on TiO_2 and stainless steel, and the coated surface showed excellent antifouling properties upon exposure to human blood and bacteria.

Besides PEG brushes for antifouling applications, PEG-based hydrogels have also been reported. Magin *et al.*[19] prepared hydrogels of poly(ethylene glycol) dimethacrylate (PEGDA), PGEDA-*co*-glycidyl methacrylate, or PEGDA-*co*-hydroxyethyl methacrylate in the form of freestanding films or coatings by a molding route, and all the hydrogels reduced significantly the initial attachment of zoospores of the green alga *Ulva linza*, cells of the diatom *Navicula incerta*, and the bacterium *Cobetia marina*. Lundberg *et al.*[20] prepared PEG-based hydrogel coatings with various hydrolytic stabilities via photocured thiol-ene chemistry and demonstrated improved antifouling performance with longer PEG chains. Browning *et al.*[21] compared the degradation of ultraviolet (UV) cured PEG diacrylamide hydrogel and PEGDA hydrogel and demonstrated the hydrolysis of the end-group acrylate esters for the *in vivo* degradation mechanism of PEGDA hydrogel. Ekblad *et al.*[22] prepared a hydrogel coating by free-radical polymerization on silanized glass, and this coating inhibits the settlement of a wide range of fouling organisms.

Although PEG brushes or PEG-based hydrogels demonstrated good antifouling performance, both of these structures have some defects from the viewpoint of engineering applications.[23–26] PEG brushes are so thin that they can be quickly depleted in service. As for the PEG-based hydrogel, there is a contradiction between hydrophilicity and underwater durability. Those PEG-based hydrogels with high hydrophilicity strongly absorb water and can be easily damaged underwater.

Recently, Kuroki *et al.*[27] reported a three-dimensional (3D) grafting strategy to produce an antifouling surface with long-lasting service life. In their reports, PEG segments were grafted not only to the surface of poly(vinylpyrrolidone) (PVP) film but also to the interior of the PVP film. Our group[28] simplified the 3D-grafting process and realized 3D grafting of PEG-b-PHEMA-b-PMPC triblock copolymers on precured acrylic-based polyurethane coatings. The coatings displayed good self-healing performance when they were immersed in a buffer solution or mechanically abraded. These primary research studies suggested that the 3D-grafting strategy may have high potential for hydrophilic polymers to establish new coating structures with high durability.

In this study, we employed a UV-curing technique to create a 3D-grafted PEG layer on polymer supports. Specifically, casting of a PEGDA layer on a UV-curable bisphenol A epoxy acrylate (BEA) sheet, interdiffusion, and UV irradiation were done in order. The process is facile and environmentally friendly, which are favorable for practical applications. The water resistance of the PEGDA-grafted BEA sheets was compared with that from the blending method, and their antifouling performance in the sea was primarily evaluated. This work extends the technique to establish a 3D-grafted polymer layer and is significant for the construction of nontoxic marine antifouling coatings.

EXPERIMENTAL

Materials

BEA resin (UV3216, 42,000–82,000 mPa·s) was purchased from Shanxi Xi Lai Wu Industrial Co. (Xi'an, China). PEGDA oligomers with molecular weights of 400 and 600 g/mol (48 and 90 mPa·s at 24 °C, respectively) were purchased from Liyang Hengyang Chemical Co. (Liyang, China), and PEGDA with a molecular weight of 1000 g/mol (solid at room temperature) was purchased from Aladdin (Shanghai, China). Photoinitiator 184 (1-hydroxycyclohexyl phenyl ketone) was purchased from Shanghai Baorun Chemical Co. (Shanghai, China). All raw materials were used as received.

Preparation of PEGDA-Grafted BEA Sheets

UV3216 (4.0 g) and photoinitiator 184 (0.103 g) were weighed into a plastic petri dish (diameter: 50 mm). The petri dish was put on a marble horizontal platform, which was placed in a constant temperature/humidity chamber [75 °C and 30% relative humidity (RH)] in advance. After 40 min of storage, the resin with the dissolved photoinitiator was leveled off and then was cooled down to room temperature to act as the polymer support.

After that, 4.0 g of PEGDA was added to the petri dish. The petri dish was moved to a constant temperature/humidity

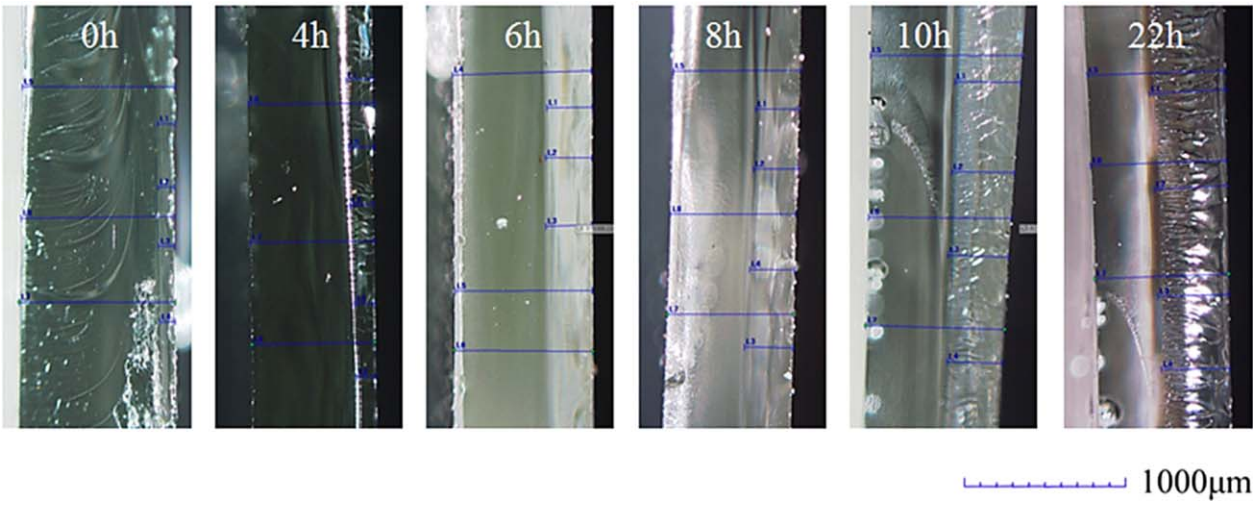

Figure 2. Photos of the cross sections of PEGDA1000-grafted BEA sheets at different interdiffusion times. [Color figure can be viewed in the online issue, which is available at wileyonlinelibrary.com.]

chamber (25 °C and 30% RH) again and stored therein for different times (0–22 h) to allow interdiffusion between the PEGDA layer and the BEA support. After a certain time, the top fluid layer was poured off. Then, the BEA base coat with the PEGDA diffused was cured via UV irradiation (2 kW) for 40 s. It should be noted that PEGDA1000 was heated to 40 °C before casting on the BEA support because it was a solid at room temperature. The interdiffusion procedure was also carried out at 40 °C for PEGDA1000.

For the sake of comparison, PEGDA and UV3216 with different mass ratios (totaling 5 g in weight) were mixed. Photoinitiator 184 (0.128 g) was further added to the mixture to get the UV-curable coatings. The coatings were then poured into a petri dish and UV-irradiated to get the blend sheets.

Characterization

The water contact angle (WCA) of UV-cured PEGDA-grafted epoxy sheets was measured by a contact angle analyzer (OCA15 Dataphysics, Filderstadt, Germany). An average value from five parallel measurements was taken. To ensure the full wetting with the surface, the WCA was recorded after the water droplet was placed on the surface for 1 min. The surface and cross section morphologies of PEGDA-grafted BEA sheets or PEGDA/BEA blend sheets were observed by an optical microscope (KH-700, Hirox, Tokyo, Japan), and the samples were photographed with a 5 megapixel camera. The viscosity of PEGDA was measured by a rotary viscometer (NDJ-1, Shanghai Sendi Scientific Instruments and Equipments Co., Shanghai, China).

The surface composition of the PEGDA-grafted epoxy sheets was monitored by attenuated total reflectance Fourier transform infrared (ATR-FTIR) spectroscopy (Vertex 70, Bruker, Ettlingen, Germany) in the range of 4000 cm^{-1} to 400 cm^{-1} with a resolution of 4 cm^{-1} and 32 scans.

Underwater Stability Tests

The underwater stability of both 3D-grafted BEA sheets and PEGDA/BEA blend sheets was tested by immersing them in deionized water. For PEGDA-grafted BEA sheets, each sheet was divided into two pieces in order to observe their cross sections easily. One piece of the sheet was immersed in deionized water. After a certain time interval, the appearance and the cross section of the sheet was observed and the WCA of the sheet was measured. Before WCA measurement, the sheets were dried in the air for 0.5–1.0 h. The WCA was recorded after an equilibrium wetting time of 10 min. To avoid fast evaporation of the water droplets during the long period of wetting, a petri dish was used to cover the water droplets. The blended sheets peeled off from the petri dish were directly immersed in the deionized water, and the change in the sheets was periodically inspected.

Antifouling Tests

Antifouling tests were carried out in the sea at Gouqi Island, Zhejiang, China. The PEGDA-grafted BEA sheets were adhered to a poly(vinyl chloride) panel, and the panel was then

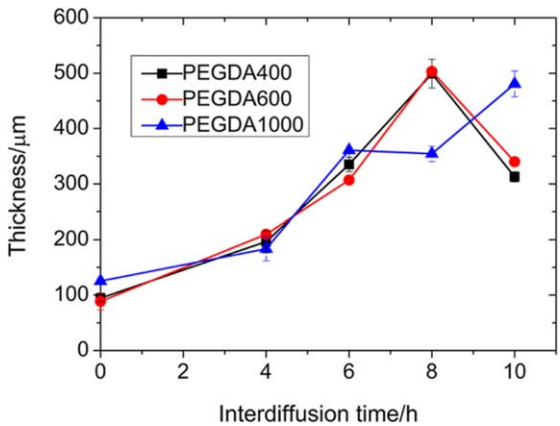

Figure 3. Change of thickness of 3D-grafted layers with interdiffusion time. [Color figure can be viewed in the online issue, which is available at wileyonlinelibrary.com.]

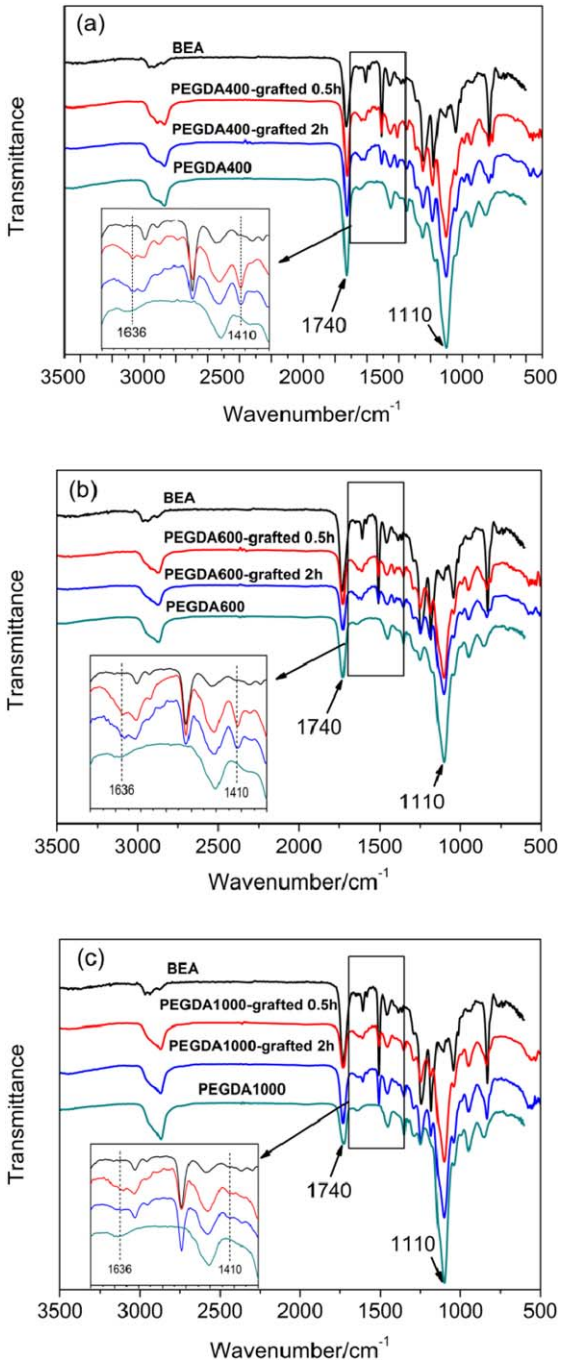

Figure 4. ATR-FTIR spectra of (a) BEA sheet, PEGDA400-grafted BEA sheets, and UV-cured PEGDA400; (b) BEA sheet, PEGDA600-grafted BEA sheets, and UV-cured PEGDA600; and (c) BEA sheet, PEGDA1000-grafted BEA sheets, and UV-cured PEGDA1000. [Color figure can be viewed in the online issue, which is available at wileyonlinelibrary.com.]

submerged at a depth of 1.0 m below the sea surface. The adhesion of marine creatures was observed with the naked eye and photographed using a camera. Two batches of shallow submergence were done for the PEGDA-grafted BEA sheets as well as the control samples. One batch spanned from August 8, 2015, to September 8, 2015, and the other from September 25, 2015 to November 25, 2015.

RESULTS AND DISCUSSION

Preparation of PEGDA-Grafted BEA Sheets

Organic coatings are usually multilayer systems in practical applications. We first tried to get 3D-grafted coatings by casting a layer of BEA base coat and subsequently a layer of PEGDA on the base coat. Unfortunately, the liquid PEGDA destroyed the thin BEA base coat. Nevertheless, if the BEA base coat was thick enough, double-layer systems can be easily established. Therefore, PEGDA was coated on thick BEA sheet in our research. The thick BEA sheet was also favorable for inspection of the diffusion of PEGDA within BEA. Before casting the PEGDA layer, the BEA base coat was first warmed to 75 °C in order to lower its viscosity for good leveling and then cooled down to room temperature.

After casting the PEGDA layer, the system was stored for a certain time to allow the interdiffusion between PEGDA and BEA. Then, the system underwent UV irradiation to be cured. To our surprise, the top PEGDA layer can also be transformed into a solid even if it did not contain a photoinitiator. It is suggested that some of the photoinitiator inside the BEA base coat diffused into the PEGDA layer. As a result, three layers, a BEA layer, an interdiffusion layer (the 3D-grafted layer), and a PEGDA layer, were formed after UV curing. However, because

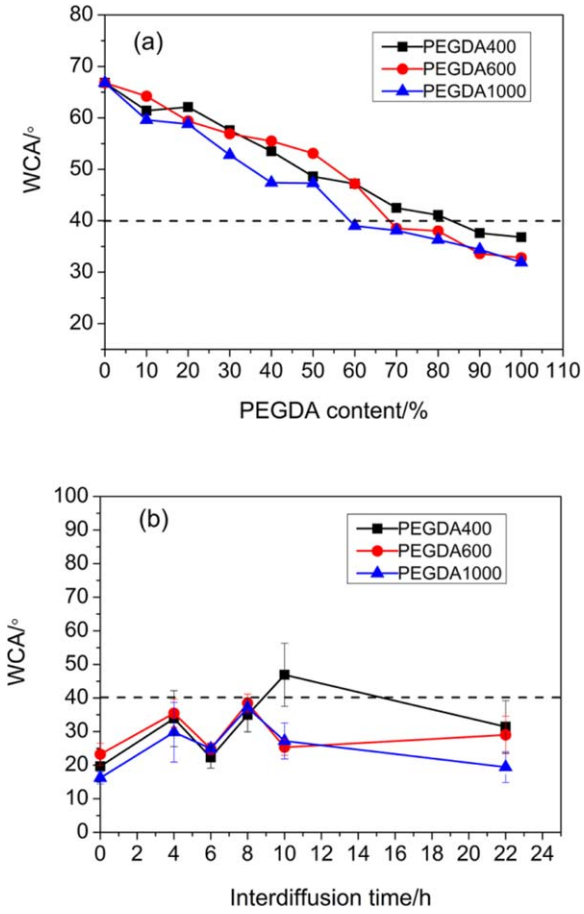

Figure 5. The WCAs of (a) PEGDA/BEA blend sheets with different PEGDA contents and (b) PEGDA-grafted BEA sheets at different interdiffusion times. [Color figure can be viewed in the online issue, which is available at wileyonlinelibrary.com.]

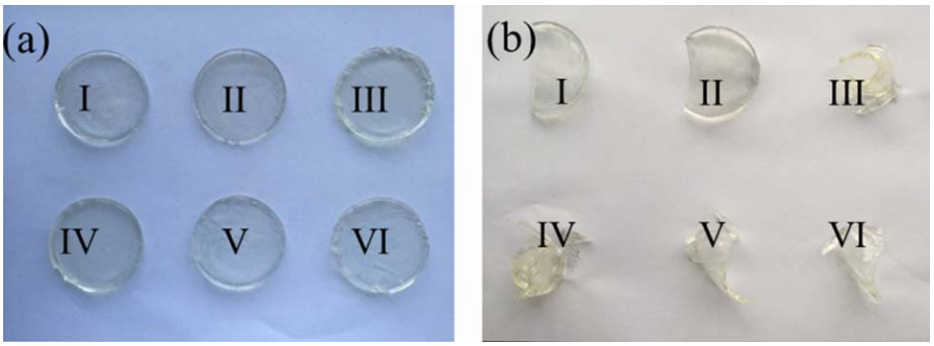

Figure 6. Photos of PEGDA-grafted BEA sheets (a) before water-resistance tests and (b) after water-resistance tests (immersion in deionized water for 7 days) for the samples (I) and (II) PEGDA-grafted BEA sheets prepared with the pouring step, (III) and (IV) PEGDA-grafted BEA sheets prepared without pouring but using the photoinitiator-containing PEGDA, and (V) and (VI) PEGDA-grafted BEA sheets prepared without either the pouring step or the photoinitiator in PEGDA. [Color figure can be viewed in the online issue, which is available at wileyonlinelibrary.com.]

of strong swelling with water, the PEGDA layer was easily peeled off when the sheet was immersed in deionized water. To eliminate this phenomenon, the top liquid layer was poured off before UV curing. The final procedure for preparation of the PEGDA-grafted BEA sheet as well as the formation mechanism of the 3D-grafted layer based on a UV curing technique is schematically described in Figure 1.

Figure 2 shows the typical cross sections of PEGDA1000-grafted BEA sheets obtained at different interdiffusion times. Even at "0 h" (that is, the PEGDA layer was poured off once the casting of PEGDA was finished) of interdiffusion time, a thin layer with a thickness of about 100 μm was obtained. This layer should be mainly caused by the adhesion of PEGDA to the BEA support. As expected, the top layer grows thicker with increasing interdiffusion time. It grew to 500 μm at 22 h interdiffusion time. Similar phenomena were observed for the cases with PEGDA400 and PEGDA600. These facts demonstrated the successful 3D grafting of PEGDA on the BEA sheet.

The thickness of the 3D-grafted layer with interdiffusion time was plotted in Figure 3 for all three series of PEGDA-grafted

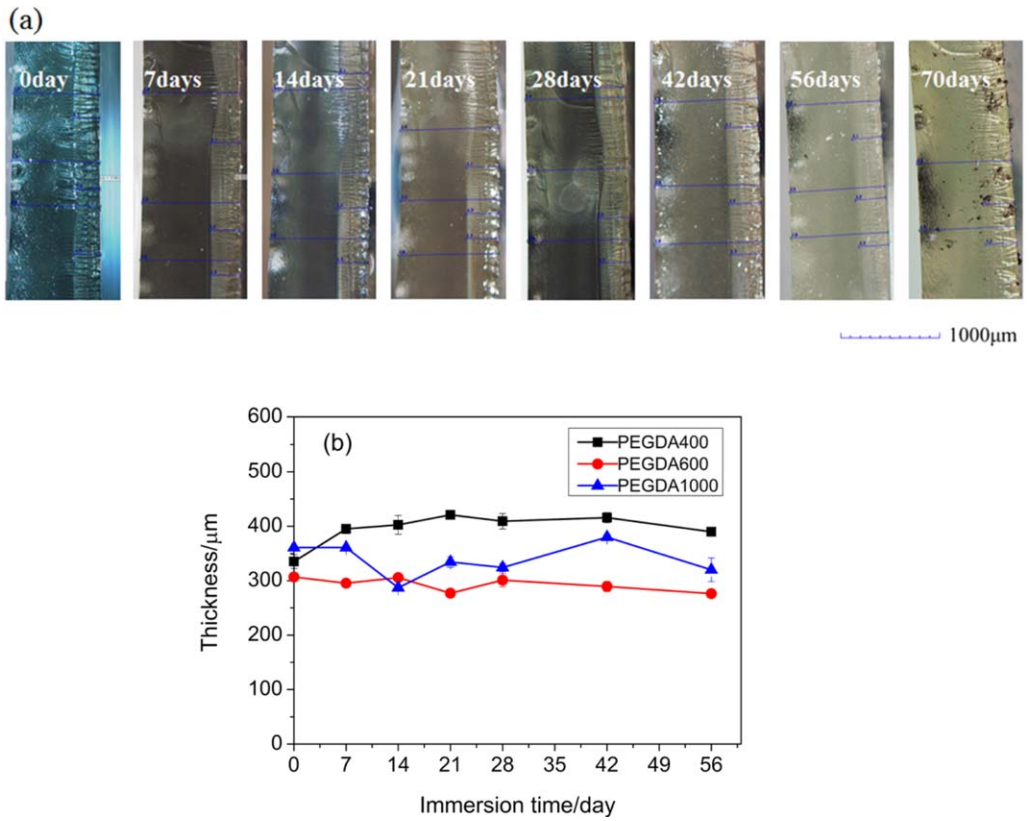

Figure 7. Evolution of thickness of the 3D-grafted layer (obtained after 6 h of interdiffusion) with immersion time: (a) cross-sectional view of PEGDA400-grafted BEA sheets during water-resistance tests and (b) the thickness of the 3D-grafted layer as a function of immersion time. [Color figure can be viewed in the online issue, which is available at wileyonlinelibrary.com.]

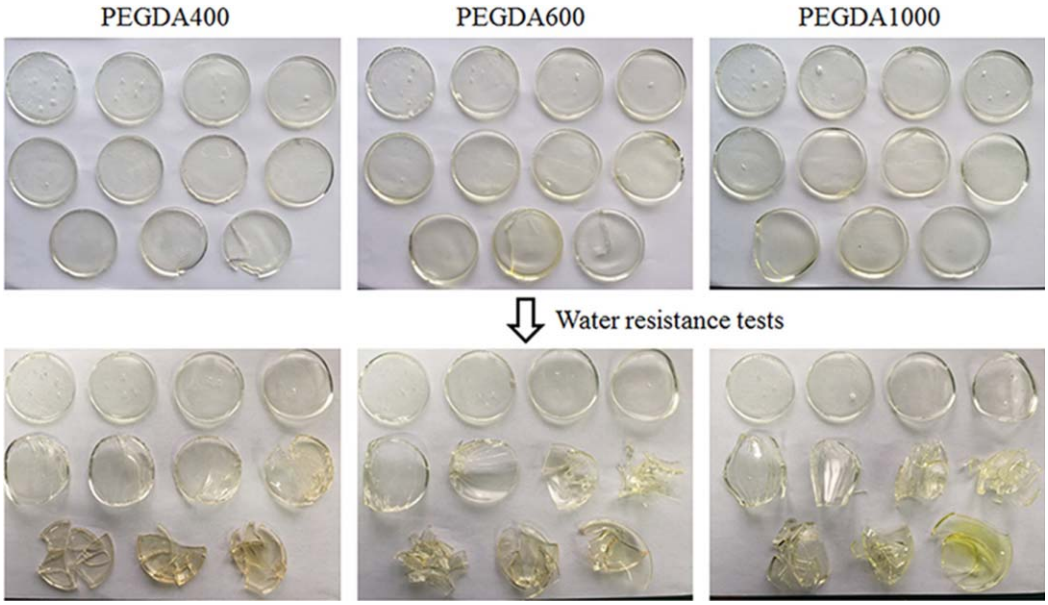

Figure 8. Photos of blend sheets with different PEGDA contents before and after water-resistance tests. From left to right and top to bottom, the PEGDA contents are 0%, 10%, 20%, 30%, 40%, 50%, 60%, 70%, 80%, 90%, and 100%, respectively. [Color figure can be viewed in the online issue, which is available at wileyonlinelibrary.com.]

BEA sheets. The thickness of the 3D-grafted layer steadily increased as the interdiffusion time increased for the PEGDA1000-grafted sample. Nevertheless, a reduction in thickness after 8 h interdiffusion time was exhibited for PEGDA400- and PEGDA600-grafted BEA sheets. This was because the upper section of the interdiffusion layer reached a low viscosity after a long interdiffusion time. Not only the PEGDA layer but also the upper section of the interdiffusion layer was poured off. Since PEGDA400 and PEGDA600 have a lower viscosity than PEGDA1000, removal of the upper section of the interdiffusion layer takes place more easily, leading to the decreased thickness of the interdiffusion layer for these two cases.

ATR-FTIR analysis was performed to probe the surface composition of the PEGDA-grafted BEA sheets. Figure 4 shows their FTIR-ATR spectra. The spectra of UV-cured PEGDA coatings and BEA sheets are also given in the figure for comparison. It can be seen that the spectra of pure PEGDA coatings with different molecular weights are similar. The profiles of the spectra of PEGDA-grafted BEA sheets are also analogous, being independent of molecular weight and interdiffusion time. All PEGDA-grafted BEA sheets show two strong absorbance peaks at 1740 cm^{-1} and 1110 cm^{-1} that are due to C═O and C─O─C groups, respectively. Since the peak at 1110 cm^{-1} in the spectrum of the BEA sheet is very weak, the peak at 1110 cm^{-1} in the spectra of PEGDA-modified sheet is reasonably attributed to PEGDA. In addition, the characteristic peaks at 1509 cm^{-1} and 832 cm^{-1} also occur in the ATR-FTIR spectra of PEGDA-grafted BEA sheets, suggesting the existence of BEA polymer in the outermost layer. This BEA polymer may be useful to enhance the surface mechanical properties of the 3D-grafted layer. In comparison with the spectra of the BEA sheet and pure PEGDA coatings, the peaks at 1636 cm^{-1} and 1410 cm^{-1} are relatively strong for all PEGDA-grafted BEA sheets, indicating incomplete UV curing.[29] This should be due to the low photoinitiator concentration in the 3D-grafted layer because of both the diffusing out of photoinitiator and the dilution with PEGDA.

The surface composition can be quantitatively understood by calculating the intensity ratio of I_{1110}/I_{1740}. The I_{1110}/I_{1740} results are as follows: 1.8, 1.8, 2.4, 2.4, 3.1, and 2.6 correspond to the samples PEGDA400-grafted-0.5h, PEGDA400-grafted-2h, PEGDA600-grafted-0.5h, PEGDA600-grafted-2h, PEGDA1000-grafted-0.5h, and PEGDA1000-grafted-2h (0.5h and 2h denote the interdiffusion time). These data show that the interdiffusion time has little effect on the surface composition for the same PEGDA. Nevertheless, more PEG segments are enriched at the surface for the sheets grafted with higher molecular weight PEGDA. This must be due to the longer length of the PEG segments between the two terminal acrylate units for the higher molecular weight PEGDA.

Wettability of PEGDA-Grafted BEA Sheets and PEGDA/BEA Blend Sheets

The WCAs of both the PEGDA/BEA blended sheets and the PEGDA-grafted BEA sheets were measured, as shown in Figure 5. The BEA sheet has a WCA of 67°, and UV-cured PEGDA400, PEGDA600, and PEGDA1000 have WCAs of 36.8°, 32.8°, and 31.9°, respectively. In other words, UV-cured PEGDA possesses a more hydrophilic surface relative to the BEA sheet. Figure 5 additionally shows that the WCA linearly decreases with increasing PEGDA content for all three series of blend sheets. Nevertheless, PEGDA1000 is more efficient in increasing the surface hydrophilicity than the other two PEGDAs. The WCA below 40 ° is reached only when the

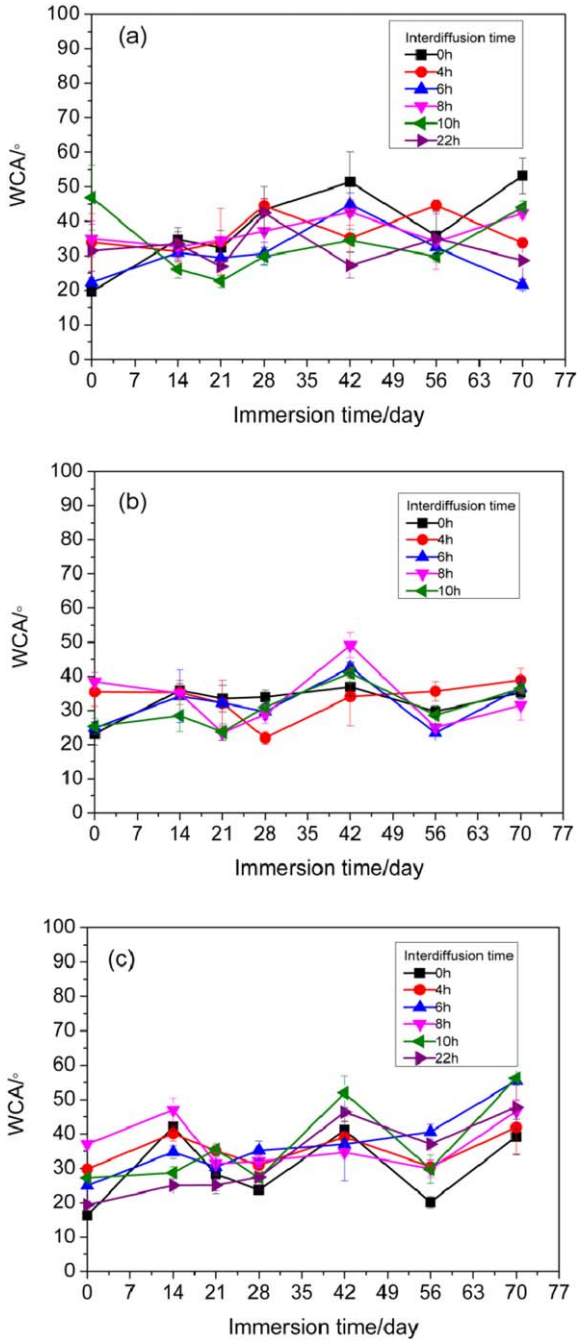

Figure 9. The WCAs of (a) PEGDA400-grafted BEA sheets, (b) PEGDA600-grafted BEA sheets, and (c) PEGDA1000-grafted BEA sheets as a function of immersion time. [Color figure can be viewed in the online issue, which is available at wileyonlinelibrary.com.]

PEGDA400, PEGDA600, and PEGDA1000 contents exceed 83 wt %, 68 wt %, and 58 wt %, respectively. These PEGDA contents are quite high.

The WCAs of PEGDA-grafted BEA sheets are always lower than 40° (except for the PEGDA400-grafted BEA sheet at 10 h interdiffusion time), regardless of the molecular weight of PEGDA. Considering that the PEGDA content in the sheet is much lower than the feeding percentage of 50 wt % (most of the PEGDA was poured off after diffusion), the 3D-grafting strategy is highly efficient in attaining a highly hydrophilic surface relative to the blending method. The lowest WCAs, 16°, 20°, and 23°, corresponding to PEDGA400-, PEGDA600-, and PEGDA1000-grafted BEA sheets, are achieved at 0 h interdiffusion time for all three series because the top layer of the sheet is composed of nearly pure PEGDA. These WCAs are even lower than their pure UV-cured PEGDA coats. This may be attributed to their low UV-curing degree since no photoinitiator was added to the PEGDA. The PEGDA layer was cured only by the photoinitiator from the BEA base. Nevertheless, little photoinitiator was diffused into the PEGDA layer at 0 h interdiffusion time. In addition, the WCAs fluctuate with interdiffusion time, which may be due to the difficult control of the pouring step.

Underwater Stability of PEGDA-Grafted BEA Sheets

The underwater stability of the PEGDA-grafted BEA sheets prepared with different 3D-grafting processes, that is, the process with and without the pouring step or the PEGDA with and without photoinitiator, was examined, as shown in Figure 6. Sheets I and II prepared with the pouring step have no change after immersion in deionized water for 7 days. However, severe curling and cracking took place for sheets III, IV, V, and VI, in which the top PEGDA layer was not removed, whether the PEGDA contained photoinitiator or not. The damage was caused by the strong swelling-induced stress within these samples. Therefore, pouring off the top PEGDA was necessary here, as mentioned above.

The appearance, cross section morphology, surface wettability, and the surface composition are all examined to understand the durability of PEGDA-grafted epoxy sheets in deionized water. Figure 7(a) shows the typical cross section of the PEGDA400-grafted BEA sheets after different numbers of days of immersion in water. The 3D-grafted layer does not swell after immersion in water. Moreover, the thickness of the 3D-grafted layer stays nearly constant as the immersion time goes up to 70 days. This

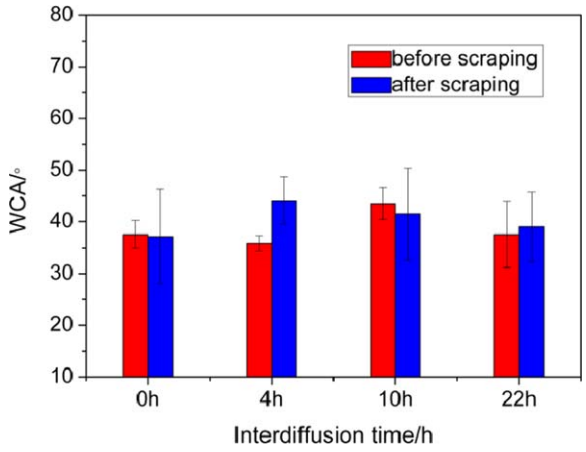

Figure 10. WCAs of PEGDA1000-grafted BEA sheets before and after scraping. [Color figure can be viewed in the online issue, which is available at wileyonlinelibrary.com.]

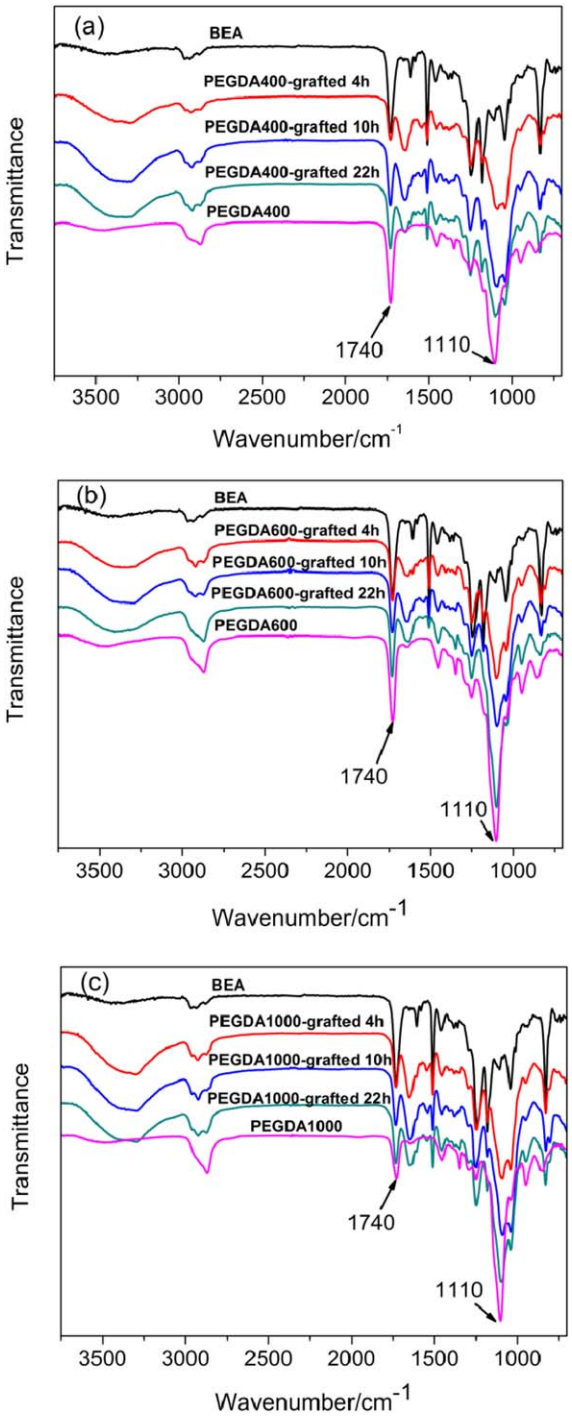

Figure 11. ATR-FTIR spectra of (a) PEGDA400-grafted BEA sheets, (b) PEGDA600-grafted BEA sheets, and (c) PEGDA1000-grafted BEA sheets after 70 days of water-resistance tests. [Color figure can be viewed in the online issue, which is available at wileyonlinelibrary.com.]

fact suggests the excellent stability of the PEGDA-grafted BEA sheet in deionized water. The thicknesses of the 3D-grafted layer for PEGDA600- and PEGDA1000-grafted BEA sheets were also monitored with immersion time. All of them are plotted in Figure 7(b). Being similar to PEGDA400-grafted epoxy sheet, their thickness does not exhibit an obvious change. These results further demonstrate the excellent water resistance of 3D-grafted BEA sheet.

The stability of the PEGDA/BEA blend sheet in water was also examined for comparison. Figure 8 shows their photos before and after underwater stability tests. Even after 7 days of tests, the blend sheets with PEGDA400, PEGDA600, and PEGDA1000 all started to crack at 40 wt % and were seriously destroyed at 80 wt %, 60 wt %, and 50 wt %, respectively. Recalling Figure 5, it is found that the blend sheets with a highly hydrophilic surface (WCA $< 40°$) are easily damaged, despite the molecular weight of PEGDA. In other words, the blending method cannot produce polymer sheets with both high hydrophilicity and excellent underwater stability. In contrast, the 3D-grafting method can do it, as described above.

The WCAs of PEGDA-grafted BEA sheets after underwater stability tests were also measured. During WCA measurement, it was found that the water droplet cannot reach equilibrium wetting within a short time. This phenomenon may be due to the aging-induced recovery of hydrophobicity in the drying step. To ensure the full wetting of the surface, a long equilibrium time, 10 min, was thus adopted. A petri dish was additionally used to cover the water droplets to alleviate water evaporation during the long equilibrium time. Figure 9 shows the WCAs of PEGDA-grafted BEA sheets as a function of immersion time. Within 70 days of underwater stability tests, PEGDA-grafted BEA sheets still displayed WCAs below 40° for most cases. Some samples have seriously fluctuating WCA data, possibly caused by the difficulty in accurate control (temperature, humidity, and so on) of the drying step and the equilibrium wetting step. These results further demonstrate the excellent stability of the PEGDA-grafted BEA sheet in deionized water and show the great potential for their application underwater.

The PEGDA1000-grafted BEA sheets after 70 days of water-resistance testing were further scraped by a razor blade, and then their WCAs were determined. The thickness of the scraped materials was about 50 μm. Figure 10 compares their WCAs before and after scraping. The wettability changed little, further demonstrating on one hand the 3D character of the grafted PEG layer and on the other hand the excellent stability of the 3D-grafted layer in water.

Figure 11 shows the ATR-FTIR spectra of the UV-cured BEA sheet, UV-cured PEGDA coatings, and PEGDA-grafted BEA sheets that had undergone 70 days of underwater stability tests. The absorbance band at 1110 cm^{-1} due to C—O—C is clearly shown for all PEGDA-grafted BEA sheets, indicating the existence of the PEG segment in these samples. The intensity ratio of I_{1110}/I_{1740} was also calculated to quantitatively understand the surface composition. For the PEGDA400-grafted BEA sheets, the I_{1110}/I_{1740} ratios are 2.5, 2.2, and 2.0 for the samples prepared with interdiffusion times of 4, 10, and 22 h, respectively, whereas, for the PEGDA600-grafted BEA sheets, these values are correspondingly 2.3, 2.6, and 2.8. As for the PEGDA1000-grafted BEA sheets, the I_{1110}/I_{1740} ratios of the samples grafted-2h, grafted-5h, and grafted-6h are 2.8, 3.1, and 3.1, respectively. As a whole, there was an increasing tendency in the I_{1110}/I_{1740}

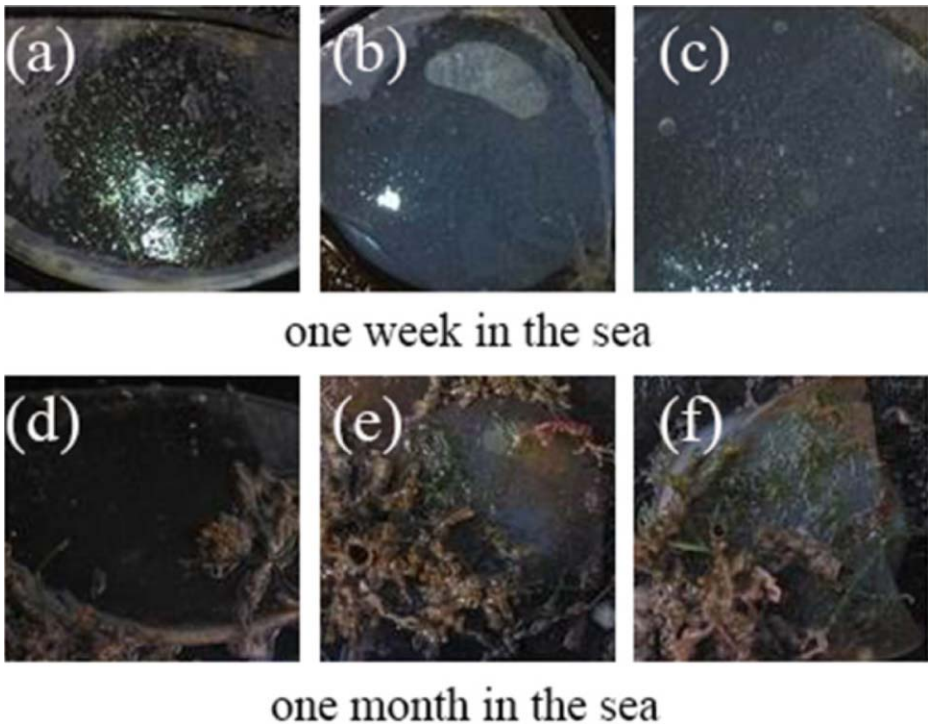

Figure 12. Biofouling communities on the samples after antifouling tests at shallow submergence in high seawater temperature in August 2015: (a,d) BEA sheet; (b,e) PEGDA1000-grafted BEA sheet without water-resistance test; and (c,f) PEGDA1000-grafted BEA sheet after water-resistance test. [Color figure can be viewed in the online issue, which is available at wileyonlinelibrary.com.]

ratio with increasing molecular weight of PEGDA. This result is rational in that PEGDA with a higher molecular weight contains more PEG segments. Additionally, in comparison with the samples before the water-resistance tests, the I_{1110}/I_{1740} ratios did not change obviously after the water-resistance tests, except for the PEGDA400-grafted BEA sheets. Enrichment of PEG segments in PEGDA400-grafted BEA sheets took place after water immersion tests presumably because the initial coverage of PEG segments at the surface was less complete. Water-induced transfer of PEG segments thus more easily emerged for these samples. Therefore, the thickness of the 3D-grafted layer, the wettability, and the surface composition all demonstrate that the PEGDA-grafted BEA sheets are durable underwater.

Antifouling Performance of PEGDA-Grafted BEA Sheets in the Sea

To check the antifouling performance in a real environment, the PEGDA-grafted epoxy sheets were submerged in the sea. Some of the sheets were first tested at shallow submergence at high water temperature (in August 2015). The micro- and macrofouling organisms on the sheets are shown in Figure 12 after immersion for 1 week and 1 month. After 1 week, the presence of microfouling organisms was not observed visually for PEGDA1000-grafted BEA sheets with and without water-resistance tests, while microfouling communities were obviously observed on the control BEA sheet surfaces. These phenomena primarily demonstrated the good antifouling performance of the PEGDA-grafted BEA sheets in the natural marine environment. That should be owed to the enrichment of PEG segments at the surface of the sheets. After immersion for 1 month, macrofouling organisms were observed visually on all surfaces of the PEGDA-grafted BEA sheets and the control. The loss of long-term antifouling performance of PEGDA1000-grafted BEA sheets may be attributed to hydrolysis[21] in weak alkaline seawater or the biodegradation of PEG segments by some bacteria in the ocean, such as *Pseudomonas* O-3,[30] *Flavobacteriumsp*,[31] and *P. vesicularis PD*.[31]

The antifouling testing in shallow submergence was also conducted at relatively low seawater temperature (September to November, 2015). Figure 13 presents the fouling organisms that settled on the samples before and after testing. After 1 month immersion, marine macrofouling organisms were obviously found on the surface of the PEGDA400-grafted BEA sheets, while few macrofouling organisms were observed on the surfaces of the PEG600-grafted BEA sheet, the PEG1000-grafted BEA sheet, and the control BEA sheet. In addition, few microfouling organisms were adhered to the PEGDA600- and PEGDA100-grafted BEA sheets when compared with those on the control BEA sheet. After immersion for two months, marine macroorganisms were attached to all sheets, and more fouling communities were found on the BEA sheet and the PEG400-grafted BEA sheet. The above tests suggest that grafted PEGDA works in antibiofouling only if the PEG segments are sufficiently long. The long-term antifouling performance of the PEGDA-grafted BEA sheets were not obtained, which should be due to the complexity and multiformity of marine biofouling. Three-dimensional grafting of more hydrophilic polymers on various

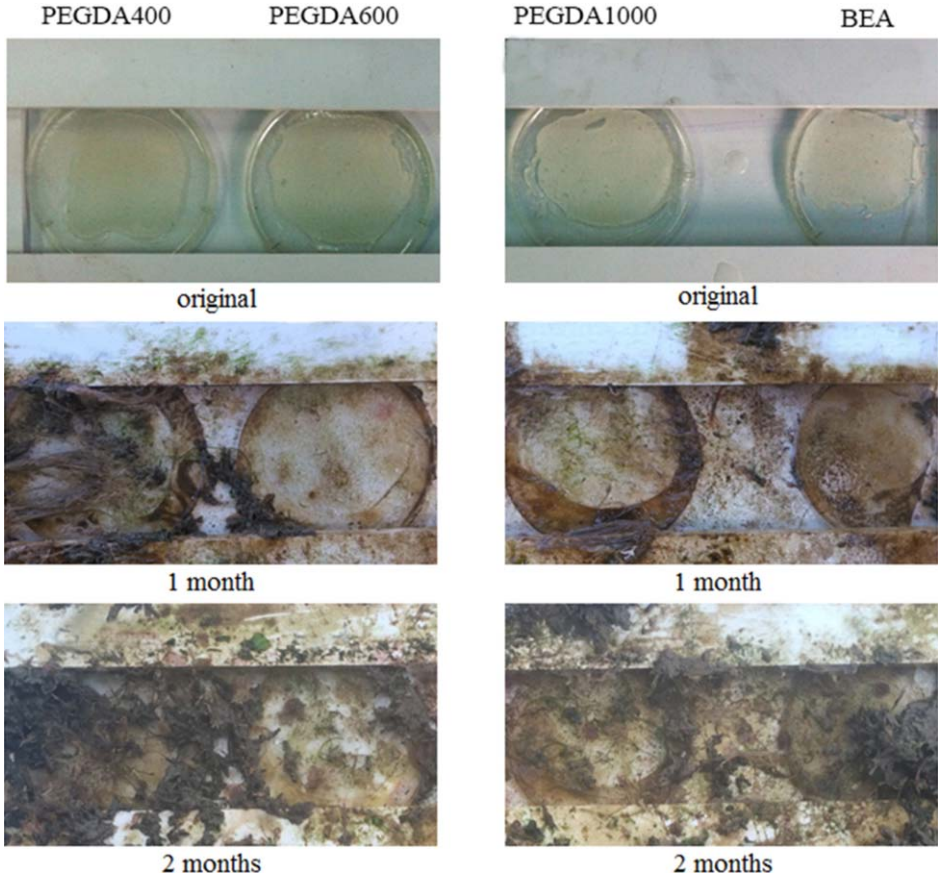

Figure 13. Biofouling communities of the samples (from left to right: PEG400-grafted BEA sheet, PEG600-grafted BEA sheet, PEGDA1000-grafted sheet, pure BEA sheet) after antifouling tests at shallow submergence in relatively low seawater temperature (from September 25 to November 25, 2015). [Color figure can be viewed in the online issue, which is available at wileyonlinelibrary.com.]

polymer supports via a UV curing technique will be tried further in order to thoroughly understand the biofouling behavior on highly hydrophilic polymer surfaces in a natural marine environment.

CONCLUSIONS

Three-dimensional grafting of PEGDA with molecular weights of 400, 600, and 1000 g/mol to a BEA sheet was successfully achieved via a UV-curing technique. Moreover, the thickness of the 3D-grafted layer can be controlled by the interdiffusion time. The 3D-PEGDA-grafted BEA sheets displayed highly hydrophilic surfaces with WCAs below 40 °, despite the molecular weight of PEGDA and the interdiffusion time. Monitoring of the thickness of the 3D-grafted layer, the wettability, and the surface composition of PEGDA-grafted BEA sheets indicated that the 3D-grafted layer was very stable in water, which is favorable for underwater applications. In contrast, the PEGDA/BEA blend sheets with highly hydrophilic surfaces were quickly damaged underwater because of strong swelling. The PEGDA1000-grafted BEA sheet exhibited good antifouling performance in a natural marine environment. Nevertheless, long-term antifouling performance was not achieved, presumably being due to the hydrolysis or biodegradation of the PEG segments. Three-dimensional grafting of other hydrophilic polymers on various polymer supports needs to be further tested to achieve long-term antifouling performance. This work does extend the methods to establish 3D-grafted polymer layers and will be significant for the construction of nontoxic antifouling coatings for underwater applications.

ACKNOWLEDGMENTS

The authors gratefully acknowledge the funding support from the specialized fund of Doctoral Program of Higher Education of China (20130071110002) and National Natural Science Foundation of China (No. 41476131).

REFERENCES

1. Gu, Y. J.; Zhou, S. X. In Novel Marine Antifouling Coatings: Antifouling Principles and Fabrication Methods; Wu, L. M.; Baghdachi, J., Eds.; John Wiley & Sons: Hoboken, New Jersey, **2015**; Chapter 11, pp 296–313.
2. Amiji, M.; Park, K. J. *Biomater. Sci., Polym. Ed.* **1993**, *4* (3), 217.
3. Prime, K.; Whitesides, G. *Science* **1991**, *252*, 1164.
4. Bearinger, J. P.; Terrettaz, S.; Michel, R.; Tirelli, N.; Vogel, H.; Textor, M.; Hubbell, J. A. *Nature Mater.* **2003**, *2*, 259.

5. Lee, J. H.; Kopecek, J.; Andradet, J. D. *J. Biomed. Mater. Res.* **1989**, *23*, 351.
6. Yang, W. J.; Neohb, K. G.; Kangb, E. T.; Teoc, S. L. M.; Rittschofd, D. *Prog. Polym. Sci.* **2014**, *39*, 1017.
7. Liu, V. A.; Jastromb, W. E.; Bhatia, S. N. *J. Biomed. Mater. Res.* **2002**, *60*, 126.
8. Prime, K. L.; Whitesides, G. M. *J. Am. Chem. Soc.* **1993**, *115*, 10714.
9. Llanos, G. R.; Sefton, M. V. *J. Biomater. Sci., Polym. Ed.* **1993**, *4*, 381.
10. Kingshott, P.; Thissen, H.; Griesser, H. J. *Biomaterials* **2002**, *23*, 2043.
11. Higuchi, A.; Sugiyama, K.; Yoon, B. O.; Sakurai, M.; Hara, M.; Sumita, M.; Sugawara, S. I.; Shirai, T. *Biomaterials* **2003**, *24*, 3235.
12. Statz, A.; Finlay, J.; Dalsin, J.; Callow, M.; Callow, J. A.; Messersmith, P. B. *Biofouling* **2006**, *22*, 391.
13. Schilp, S.; Kueller, A.; Rosenhahn, A.; Grunzea, M.; Pettitt, M. E.; Callow, M. E.; Callowb, J. A. *Biointerphases* **2007**, *2*, 143.
14. Schilp, S.; Rosenhahn, A.; Pettitt, M. E.; Bowen, J.; Callow, M. E.; Callow, J. A.; Grunze, M. *Langmuir* **2009**, *25*, 10077.
15. Efremova, N. V.; Sheth, S. R.; Leckband, D. E. *Langmuir* **2001**, *17*, 7628.
16. He, H. T.; Jing, W. H.; Xing, W. H.; Fan, Y. Q. *Appl. Surf. Sci.* **2011**, *258*, 1038.
17. Sun, F. Q.; Li, X. S.; Xu, J. K.; Cao, P. T. *Chin. J. Polym. Sci.* **2010**, *28*, 705.
18. Khalila, F.; Franzmanna, E.; Ramckea, J.; Dakischewb, O.; Lipsb, K. S.; Reinhardtc, A.; Heisigc, P.; Maisona, W. *Colloids Surf., B* **2014**, *117*, 185.
19. Magin, C. M.; Finlay, J. A.; Clay, G.; Callow, M. E.; Callow, J. A.; Brennan, A. B. *Biomacromolecules* **2011**, *12*, 915.
20. Lundberg, P.; Bruin, A.; Klijnstra, J. W.; Nystrom, A. M.; Johansson, M.; Malkoch, M.; Hult, A. *ACS Appl. Mater. Interfaces* **2010**, *2*, 903.
21. Browning, M. B.; Cereceres, S. N.; Luong, P. T.; Cosgriff-Hernandez, E. M. *J. Biomed. Mater. Res.* **2014**, *102*, 4244.
22. Ekblad, T.; Bergstroem, G.; Ederth, T.; Conlan, S. L.; Mutton, R.; Clare, A. S.; Wang, S.; Liu, Y. L.; Zhao, Q.; D'Souza, F.; Donnelly, G. T.; Willemsen, P. R.; Pettitt, M. E.; Callow, M. E.; Callow, J. A.; Liedberg, B. *Biomacromolecules* **2008**, *9*, 2775.
23. Knoll, D.; Hermans, J. *J. Biol. Chem.* **1983**, *258*, 5710.
24. Zhu, X. Y.; Jun, Y.; Staarup, D. R.; Major, R. C.; Danielson, S.; Boiadjiev, V.; Gladfelter, W. L.; Bunker, B. C.; Guo, A. *Langmuir* **2001**, *17*, 7798.
25. Currie, E. P. K.; Norde, W.; Stuart, M. A. C. *Adv. Colloid Interface Sci.* **2003**, *100*, 205.
26. Hucknall, A.; Rangarajan, S.; Chilkoti, A. *Adv. Mater.* **2009**, *21*, 2441.
27. Kuroki, H.; Tokarev, I.; Nykypanchuk, D.; Zhulina, E.; Minko, S. *Adv. Funct. Mater.* **2013**, *23*, 4593.
28. Chen, K. L.; Zhou, S. X.; Wu, L. M. *RSC Adv.* **2015**, *5*, 104907.
29. Kang, G. D.; Cao, Y. M.; Zhao, H. Y.; Yuan, Q. J. *Membr. Sci.* **2008**, *318*, 227.
30. Suzuki, T. *Agric. Biol. Chem.* **1976**, *40*, 497.
31. Watanabe, Y.; Hamada, N.; Morita, M.; Tsujisaka, Y. *Arch. Biochem. Biophys.* **1976**, *174*, 575.